

Properties and Applications of Commercial Magnetorheological Fluids

Mark R. Jolly, Jonathan W. Bender, and J. David Carlson

Thomas Lord Research Center
Lord Corporation
110 Lord Drive
Cary, NC 27511

ABSTRACT

The rheological and magnetic properties of several commercial magnetorheological (MR) fluids are presented and discussed. These fluids are compared using appropriate figures of merit based on conventional design paradigms. Some contemporary applications of MR fluids are discussed. These applications illustrate how various material properties may be balanced to provide optimal performance.

Keywords: magnetorheological fluids, MR fluids, magnetorheological fluid dampers, MR fluid properties.

1. INTRODUCTION

Magnetorheological (MR) fluids are materials that respond to an applied magnetic field with a change in rheological behavior. Typically, this change is manifested by the development of a yield stress that monotonically increases with applied field. Interest in magnetorheological fluids derives from their ability to provide simple, quiet, rapid-response interfaces between electronic controls and mechanical systems. That magnetorheological fluids have the potential to radically change the way electromechanical devices are designed and operated has long been recognized.

MR fluids are considerably less well known than their electrorheological (ER) fluid analogs. Both fluids are non-colloidal suspensions of polarizable particles having a size on the order of a few microns. The initial discovery and development of MR fluids and devices can be credited to Jacob Rabinow at the US National Bureau of Standards (Rabinow, 1948a, 1948b, 1951) in the late 1940s. Interestingly, this work was almost concurrent with Winslow's ER fluid work. The late 1940s and early 1950s actually saw more patents and publications relating to MR than to ER fluids. Except for a flurry of interest after their initial discovery, there has been scant information published about MR fluids. Only recently has a resurgence in interest in MR fluids been seen (Shtarkman, 1991; Kordonsky, 1993; Weiss et al., 1993; Carlson et al., 1994; Carlson, 1994; Carlson and Weiss, 1994). While the commercial success of ER fluids has remained elusive, MR fluids have enjoyed recent commercial success. A number of MR fluids and various MR fluid-based systems have been commercialized including an MR fluid brake for use in the exercise industry (Anon., 1995; Chase, 1996), a controllable MR fluid damper for use in truck seat suspensions (Carlson, Catanzarite and St.Clair, 1995; Lord, 1997) and an MR fluid shock absorber for oval track automobile racing.

The magnetorheological response of MR fluids results from the polarization induced in the suspended particles by application of an external field. The interaction between the resulting induced dipoles causes the particles to form columnar structures, parallel to the applied field. These chain-like structures restrict the motion of the fluid, thereby increasing the viscous characteristics of the

suspension. The mechanical energy needed to yield these chain-like structures increases as the applied field increases resulting in a field dependent yield stress. In the absence of an applied field, MR fluids exhibit Newtonian-like behavior. Thus the behavior of controllable fluids is often represented as a Bingham plastic having a variable yield strength (e.g., Phillips, 1996). In this model, the flow is governed by Bingham's equations:

$$\tau = \tau_y(H) + \eta \dot{\gamma}, \tau \geq \tau_y \quad (1)$$

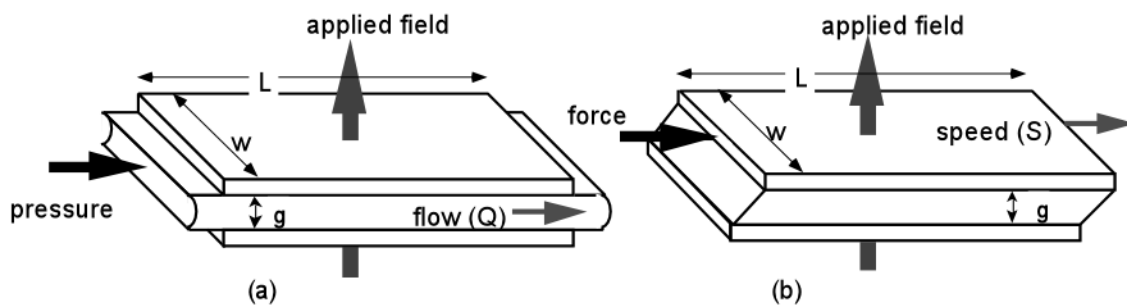
at stresses τ above the field dependent yield stress τ_y . Below the yield stress (at strains of order 10^{-3}), the material behaves viscoelastically:

$$\tau = G \gamma, \tau < \tau_y \quad (2)$$

where G is the complex material modulus. It has been observed in the literature that the complex modulus is also field dependent (Weiss, Carlson and Nixon, 1994; Nakano, Yamamoto and Jolly, 1997). While the Bingham plastic model has proved useful in the design and characterization of MR fluid-based devices, true MR fluid behavior exhibits some significant departures from this simple model. Perhaps the most significant of these departures involves the non-Newtonian behavior of MR fluids in the absence of a magnetic field (Kormann, Laun and Klett, 1994).

This paper is organized as follows. In the next section, some common MR fluid device design theory is reviewed. Simple MR fluid figures of merit based on this theory are then presented. Section 3 presents the properties of four commercially available MR fluids (Lord, 1998). Using some of these properties as a basis, figures of merit of the four MR fluids are then presented. In section 4, a few contemporary device applications of MR fluids in linear motion devices are discussed. Conclusions are presented in section 5.

2. MR DEVICE DESIGN AND FIGURES OF MERIT



2.1 Common Device Geometries

Figure 1: Basic operational modes for controllable fluid devices: (a) pressure driven flow mode, and (b) direct shear mode (after Carlson et al., 1994).

Most devices that use controllable fluids can be classified as having either fixed poles (pressure driven flow mode) or relatively moveable poles (direct-shear mode). Diagrams of these two basic operational modes are shown in Fig. 1. Examples of pressure driven flow (PDF) mode devices include servo-valves, dampers and shock absorbers. Examples of direct-shear mode devices include clutches, brakes, chucking and locking devices. A third mode of operation known as squeeze-film mode has also been used in low motion, high force applications (Jolly and Carlson, 1996).

The pressure drop developed in a device based on pressure driven flow mode is commonly assumed to result from the sum of a viscous component ΔP_η and a field dependent induced yield stress component ΔP_τ . This pressure may be approximated by (Phillips, 1969)

$$\Delta P = \Delta P_\eta + \Delta P_\tau(H) = \frac{12 \eta Q L}{g^3 w} + \frac{c \tau_y(H) L}{g} \quad (3)$$

where L , g and w are the length, gap and width of the flow channel between the fixed poles, Q is the volumetric flow rate, η is the viscosity with no applied field and τ_y is the yield stress developed in response to an applied field H . The parameter c is a function of the flow velocity profile and has a value ranging from a minimum value of 2 (for $\Delta P_\tau/\Delta P_\eta$ less than ~ 1) to a maximum value of 3 (for $\Delta P_\tau/\Delta P_\eta$ greater than ~ 100). In a like manner, the force developed by a direct-shear device is:

$$F = F_\eta + F_\tau(H) = \frac{\eta S A}{g} + \tau_y(H) A \quad (4)$$

where S is the relative pole velocity and $A=Lw$ is the shear (pole) area.

2.2 Active Fluid Volume and Device Aspect Ratio

While Equations (3) and (4) are certainly useful in the design of controllable fluid devices, they often do not provide the best insight into the significance of the various parameters. It is often useful to algebraically manipulate the above equations to provide a minimum active fluid volume (Duclos, 1988; Carlson et al., 1994):

$$V = k \left(\frac{\eta}{\tau^2} \right) \lambda W_m \quad (5)$$

where k is a constant and $V = Lwg$ can be regarded as the necessary active fluid volume in order to achieve the desired control ratio λ at a required controllable mechanical power level W_m . For pressure driven flow: $k=12/c^2$, $\lambda=\Delta P_\tau/\Delta P_\eta$ and $W_m=Q \Delta P_\tau$. For direct shear: $k=1$, $\lambda=F_\tau/F_\eta$ and $W_m=F_\tau S$. It is important to note that in both cases the minimum active fluid volume is proportional to the product of three terms: a term that is a function of fluid material properties (η/τ^2); the desired control ratio or dynamic range λ ; and the controlled mechanical power dissipation W_m sought.

By noting that for both geometries, $V = Lwg$, Equation (5) can be further manipulated to give

$$wg^2 = \frac{12}{c} \left(\frac{\eta}{\tau} \right) \lambda Q \quad (\text{pressure driven flow mode}) \quad (6)$$

$$g = \left(\frac{\eta}{\tau} \right) \lambda S \quad (\text{direct shear mode}) \quad (7)$$

These two equations provide geometric constraints and necessary aspect ratios for MR devices based on MR fluid properties, the desired control ratio or dynamic range, and the device speed (or flow). It is interesting to note that while the active fluid volume depends on the ratio of viscosity to yield stress squared (η/τ^2), the geometric constraint depends upon the ratio η/τ .

2.3 MR Fluid Figures of Merit

The mechanical and electrical power *densities* of an MR device are given by

$$\hat{W}_m = \tau \dot{\gamma} \quad (8)$$

$$\hat{W}_e = \frac{BH}{2t_c} \quad (9)$$

where $\dot{\gamma}$ is the fluid shear rate (or normalized flow rate, e.g., $\dot{\gamma} = S/g$), B and H are the magnetic flux density and field in the fluid and t_c is the characteristic time for the establishment of a magnetic field in the fluid. A fluid efficiency can now be defined as the ratio of the mechanical and electrical power densities given by:

$$\alpha = \frac{\hat{W}_m}{\hat{W}_e} = 2(t_c \dot{\gamma}) \frac{\tau}{BH} \quad (10)$$

where τ and B are defined at a common H.

From the above developments, several figures of merit can be conceived. The first is based on the active fluid volume:

$$F_1 = \frac{\tau^2}{\eta} \quad (11)$$

which is seen to be inversely proportional to the minimum active fluid volume V and has units of Pa/s. Maximizing this figure of merit will minimize device size and electrical power consumption since $W_e = \hat{W}_e V$. This figure of merit also reflects the dynamic range of a device based on a specified fluid since, for a given active fluid volume, as F_1 increases so will λ (Eq. 5). For weight sensitive applications, this figure of merit may be modified to penalize large fluid densities ρ :

$$F_2 = \frac{\tau^2}{\eta \rho} \quad (12)$$

which is inversely proportional to the minimum active fluid mass and has units of m^2/s^3 . Finally, for high bandwidth applications, a unitless figure of merit based on power efficiency (Equation 10) is given by:

$$F_3 = \frac{\tau}{B H} \quad (13)$$

Maximizing this figure of merit will minimize electrical power consumption of an MR device for a given delivered mechanical power at a desired bandwidth.

These three figures of merit provide a generic means of comparing the nominal behavior of various MR fluids. Other factors such as stability, durability and temperature range will typically have a significant impact on the suitability of an MR fluid for a particular application.

3. PROPERTIES OF COMMERCIAL MR FLUIDS

Magnetic, rheological, tribological and settling properties of four commercial MR fluids are discussed. The basic composition of these four fluids is given in Table 1.

Table 1. Basic composition and density of four commercial MR fluids (Lord, 1998).

<i>Commercial MR Fluid</i>	<i>Percent Iron by Volume</i>	<i>Carrier Fluid</i>	<i>Density (g/ml)</i>
MRX-126PD	26	Hydrocarbon oil	2.66
MRX-140ND	40	Hydrocarbon oil	3.64
MRX-242AS	42	Water	3.88
MRX-336AG	36	Silicone oil	3.47

3.1 Rheological Properties

The rheological properties of controllable fluids depend on concentration and density of particles, particle size and shape distribution, properties of the carrier fluid, additional additives, applied field, temperature, and other factors. The interdependency of all these factors is very complex, yet is important in establishing methodologies to optimize the performance of these fluids for particular applications.

The magnetorheological effect of the four MR fluids was measured on a custom rheometer using a 46 mm diameter parallel plate geometry set at a 1 mm gap. In the parallel plate geometry, shear rate varies linearly across the fluid sample with the maximum shear rate occurring at the outer radius. The rheometer is capable of applying greater than 1 Tesla through the fluid sample. Figure 2 shows the shear stress in the MR fluids as a function of flux density at a maximum shear rate of 26 s^{-1} . At such a low shear rate, this shear stress data is approximately equivalent to the fluid yield stress as defined in Eq. (1). At low flux densities, the fluid stress can be seen to exhibit a power law behavior. The approximate power law index of 1.75 lies in the range of low to intermediate field behavior predicted by contemporary models of magnetorheology. Both linear models and models accounting for nonlinear magnetic effects such as particle saturation (Ginder, Davis and Elie, 1995; Jolly, Carlson and Muñoz, 1996) predict quadratic behavior at very low flux densities. The non-linear model proposed by Ginder, Davis and Elie (1995) predicts a power law index of 1.5 at intermediate fields. Beyond flux densities of about 0.2-0.3 Tesla, the effects of magnetic saturation are revealed as a departure from power law behavior. The stress response ultimately plateaus as the MR fluids approach complete magnetic saturation. As can be seen, the flux density at which this saturation occurs increases as the iron volume fraction in the fluid increases.

In all MR fluid formulations optimized for a specific application or class of applications, the fluid viscosity in the *absence* of a field is most significantly a function of the carrier oil, suspension agents, and particle loading. The figures-of-merit described earlier are benefited by a low fluid viscosity, but must be balanced with other fluid requirements such as temperature range and particle resuspendability. Because of both the addition of suspension agents and changes in magnetic particle microstructure during shear, most MR fluids exhibit significant shear thinning.

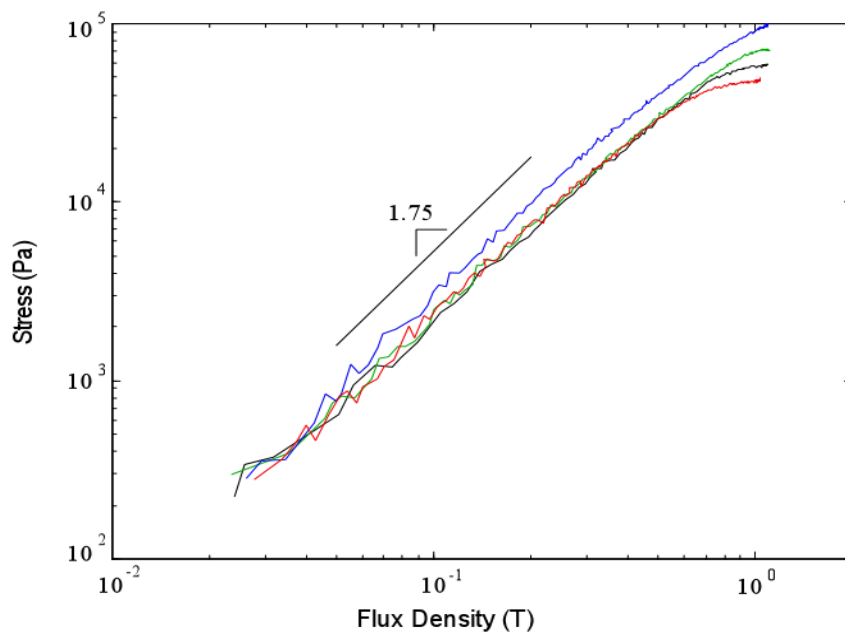


Figure 2. Fluid shear stress as a function of magnetic flux density at a maximum shear rate of 26 s⁻¹. Ascending order of the plots corresponds increasing iron volume fraction.

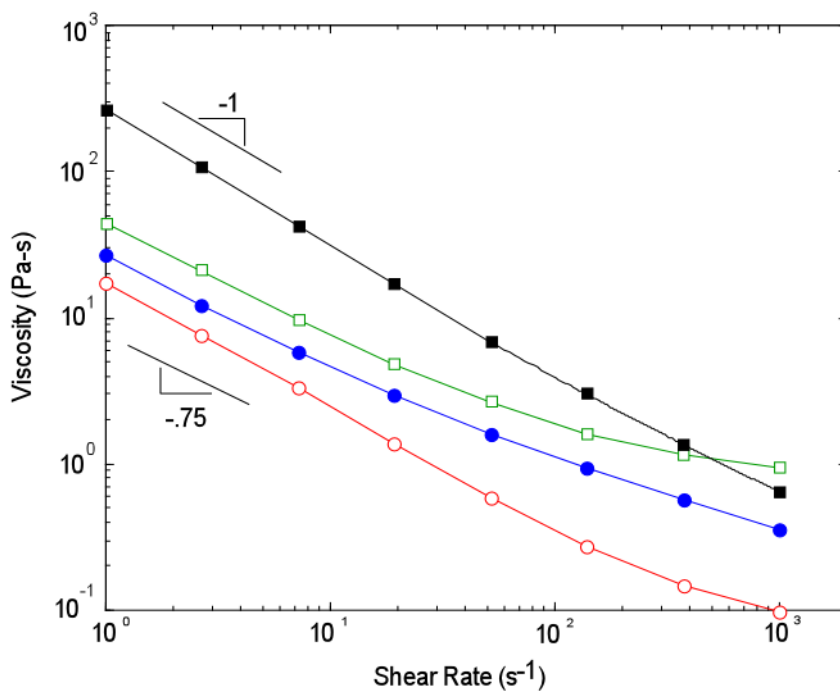


Figure 3. Viscosity as a function of shear rate at 25°C for MRX-126PD (○), MRX-242AS (●), MRX-140ND (□), and MRX-336AG (■).

The viscosity of the four MR fluids was measured on a TA Instruments CS²500 controlled stress rheometer using a cone and plate geometry (40 mm diameter and 1° cone angle). Figure 3 shows viscosity of the four MR fluids a function of shear rate. It can be seen that the fluid viscosity does not strictly scale with iron loading. Indeed, the fluid viscosity is significantly a function of the composition and chemistry of the carrier oils. The MR fluids shown are seen to exhibit low shear rate power law behavior with power law indices between -0.75 and -1. At high shear rates, the rate of shear thinning decreases and will approach an asymptotic value dictated largely by the solids loading, carrier oil viscosity, and extent of shear thinning of the suspension agents. MRX-336AG exhibits nearly an order of magnitude greater viscosity at low shear rate as compared to the other MR fluids. This is a result of a significant zero-field yielding behavior of this fluid, characterized by a -1 power law index at low shear rates. The plastic viscosity ($\partial\sigma / \partial\dot{\gamma}$) beyond the yielding regime is actually quite low ($\sim 10^{-1}$ Pa-s).

3.2 Magnetic Properties

Understanding the magnetic properties of MR fluids is important for designing MR fluid-based devices. In many such devices, the MR fluid represents the largest magnetic reluctance within the magnetic circuit. These magnetic properties may also prove useful in providing insight into the character and formation of particle structures within the fluid.

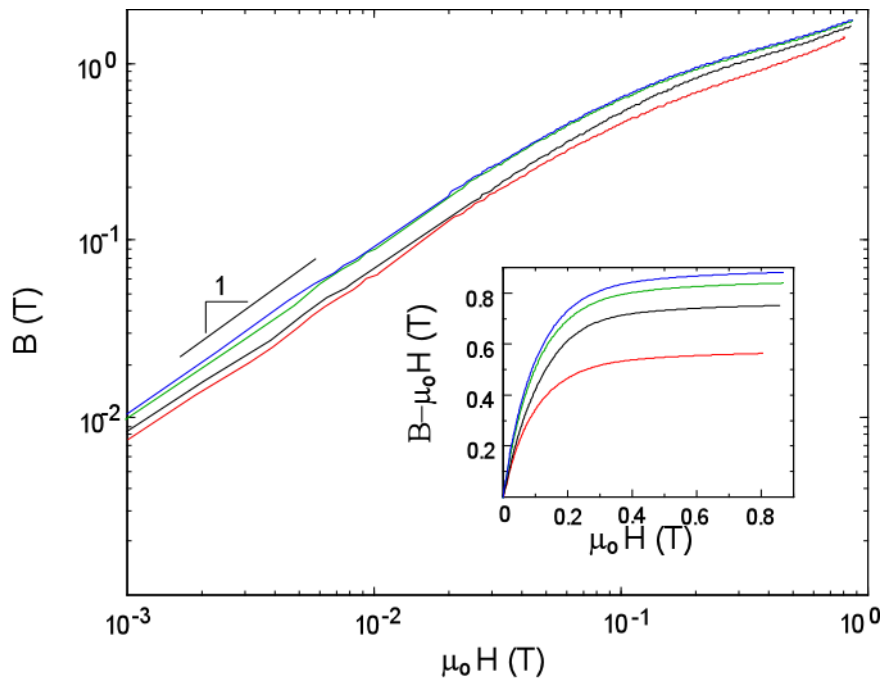


Figure 4. Flux density within MR fluids as a function of applied field. Inset: Intrinsic induction as a function of applied field. Ascending order of the plots corresponds to increasing iron volume fraction.

Magnetic induction curves, or $B-H$ curves, of the four commercial MR fluids are shown in Figure 4. As can be seen, the MR fluids exhibit approximately linear magnetic properties up to an applied field of about $0.02/\mu_0$ A/m, where $\mu_0 = 4\pi \times 10^{-7}$ T-m/A is the permeability of a vacuum. In this region, the differential permeability (the slope of $B(H)$) of the MR fluids is relatively constant. These permeabilities vary between 5 and 9 times that of a vacuum. The magnetic properties of MR fluids vary significantly from the properties of most bulk ferromagnetic properties in that ferromagnetic induction can typically be linearized over a much broader range of applied field and the corresponding permeabilities are several orders of magnitude greater. MR fluids begin to exhibit gradual magnetic saturation beyond the linear regime. Complete saturation typically occurs at fields beyond $0.4/\mu_0$ A/m. The intrinsic induction or polarization density ($B - \mu_0 H$) of an MR fluid at complete saturation is ϕJ_s Tesla, where ϕ is the volume percent of particles in the fluid and J_s is the saturation polarization of the particulate material (Jolly, Carlson and Muñoz, 1996). For example, a fluid containing 30% iron ($J_s = 2.1$ Tesla) saturates at about $(0.3)(2.1) = 0.63$ Tesla. Little or no hysteresis can be observed in the induction curves. This superparamagnetic behavior is a consequence of the magnetically soft properties of the iron used as particulate material in these fluids and the mobility of this particulate phase.

3.3 Lubricity, Settling Characteristics, and Material Compatibility

MR fluid is inherently somewhat abrasive. The degree to which it will effect the durability of a particular part or component depends on a number of factors associated with fluid composition and device design. Wear bands and other bearing materials that are exposed to MR fluid in direct sliding contact are often critical abrasion regions, particularly in linear device applications. The ability of MR fluids to lubricate conformal sliding surfaces will reflect the propensity for wear of such surfaces within MR fluid-based devices. The coefficients of friction for MR fluid lubricated iron-on-iron and nylon-on-iron conformal interfaces are given in Table 2. These were measured with an Instron Model 4204 using a standard sled geometry with contact dimensions of 7.6 cm by 7.6 cm. These results reflect the averages of multiple runs at a sled velocity of 2.6 mm/s and with varying normal forces in the range of

10 N to 20 N (no magnetic field was present). It can be seen that with MR fluid lubrication, the sliding friction is reduced by a factor of two or three over the dry interface. However, it was found that the measurement of MR fluid-lubricated sliding friction by this method exhibited somewhat poor reproducibility. This is attributed to the complex rheological properties of MR fluids implying that sliding friction properties will be a function of both sliding speed and interfacial fluid film thickness.

Table 2. Average coefficients of sliding friction for MR fluid-lubricated conformal interfaces.

<i>Commercial MR Fluid</i>	<i>Iron-on-Iron</i>	<i>Nylon-on-Iron</i>
Dry	0.18	0.19
MRX-126PD	0.04 - 0.07	0.04 - 0.07
MRX-140ND	0.07 - 0.09	0.05 - 0.07
MRX-242AS	0.05 - 0.07	0.06 - 0.07
MRX-336AG	0.08 - 0.11	0.08 - 0.11

As with any micron-scale particulate suspension in which a density mismatch between the particulate and surrounding fluid exists, settling in MR fluids must be considered when formulating. Again, the specific application dictates to what extent settling must be controlled and how it is to be measured. For example, a seismic damper application may have very strict settling requirements, whereas settling may be unimportant in a brake application. A simple, non-application specific comparison of settling has been summarized in Table 3, which tabulates the initial rate of settling as a percentage of total height of a fluid column. In this experiment, the fluids were placed in a glass graduated cylinder and left to settle for up to five weeks at room temperature. (Note that settling results in a particle-free fluid on top of a particle-rich suspension, and as settling occurs, the settling rate slows. Thus, the initial settling rate is the most rapid period of settling.) In general, settling is governed by the rheological character of the suspending medium, surface properties of the magnetic particles, and the presence of surface active agents. In a device, settling can be further influenced by the presence of remnant fields, device orientation, and aspects of the device geometry. For the fluids studied here, the fluids ranked in order of viscosity. Those with the highest viscosity (Figure 3) exhibited the lowest initial settling rate.

Table 3. Initial settling rates.

<i>Fluid</i>	<i>Initial settling rate (%/day)</i>
MRX-126PD	1.0
MRX-140ND	0.3
MRX-242AS	0.2
MRX-336AG	0.0 (non-detectable)

Other criteria governing the composition of an MR fluid include the device operating temperature range, compatibility with materials within the device, and whether or not the fluid will be sealed from the atmosphere. Table 4 contains a list of typical seal materials with which the selected fluids are checked for excessive swelling or loss in strength. (Note that this information is intended merely as a general guideline.) Of the fluids listed, water-based fluid MRX-242AS is the only fluid that should not be used in an unsealed system.

Table 4. Temperature and compatibility properties.

<i>Commercial MR Fluid</i>	<i>Temperature Range</i>	<i>Compatibility with...</i>					
		<i>Natural Rubber</i>	<i>Nitrile Rubber</i>	<i>Fluoro- elastomer</i>	<i>Silicone</i>	<i>EPDM</i>	<i>Neoprene</i>
MRX-126PD	-40°C to 150°C	poor	good	good	fair	poor	good
MRX-140ND	-40°C to 150°C	poor	good	good	fair	poor	good
MRX-242AS	5°C to 90°C	good	good	good	good	good	good
MRX-336AG	-50°C to 200°C	good	good	good	poor	good	good

3.4 MR Fluid Figures of Merit

Figure 5 shows the figure of merit $F_1 = \tau^2/\eta$ as a function of shear rate for the four MR fluids. This figure of merit reflects the dynamic range (or control ratio) of an MR device as well as required MR fluid volume and power consumption. It is seen that as shear rate increases, the four fluids exhibit significant improvements in F_1 due to the substantial shear thinning character of these fluids. A broad range of F_1 is observed amongst the MR fluids resulting from the acute dependence of F_1 on viscosity. Figure 6 shows the figure of merit $F_2 = \tau^2/\eta\rho$ as a function of shear rate. This figure of merit is closely related to F_1 except that it further penalizes fluid density. With the exception of vertical shifts in the data, F_2 demonstrates much the same character as F_1 . It is interesting to note that, as measured by F_2 , MRX-126PD is particularly well suited for low shear rate applications and MRX-242AS is better suited for high shear rate applications. Both F_1 and F_2 illustrate that MR fluids in general exhibit better rheological behavior at higher shear rates due to the shear thinning character.

The figure of merit $F_3 = \tau/BH$ as a function of flux density is shown in Figure 7 for the four MR fluids. This figure of merit is related to the power efficiency of MR fluids and is important in applications where high bandwidth is sought. The dashed lines in this data correspond to asymptotic extrapolation generated with least-squares fits. This was done as an alternative to presenting the increased level of measurement and computational noise present at lower flux densities. It can be seen that there is a steady decrease in F_3 as flux density increases with a plummet in F_3 as the MR fluid begins to magnetically saturate. Ultimately, F_3 will approach zero as the fluid approaches the condition for which increases in magnetic input cease to result in increased yield stress. The MR fluids with higher iron loading generally measure better by F_3 since iron loading results both in higher magnetic permeability and higher yield stresses. Interestingly, this proves strictly true only at higher flux densities for the four MR fluids shown in Figure 7.

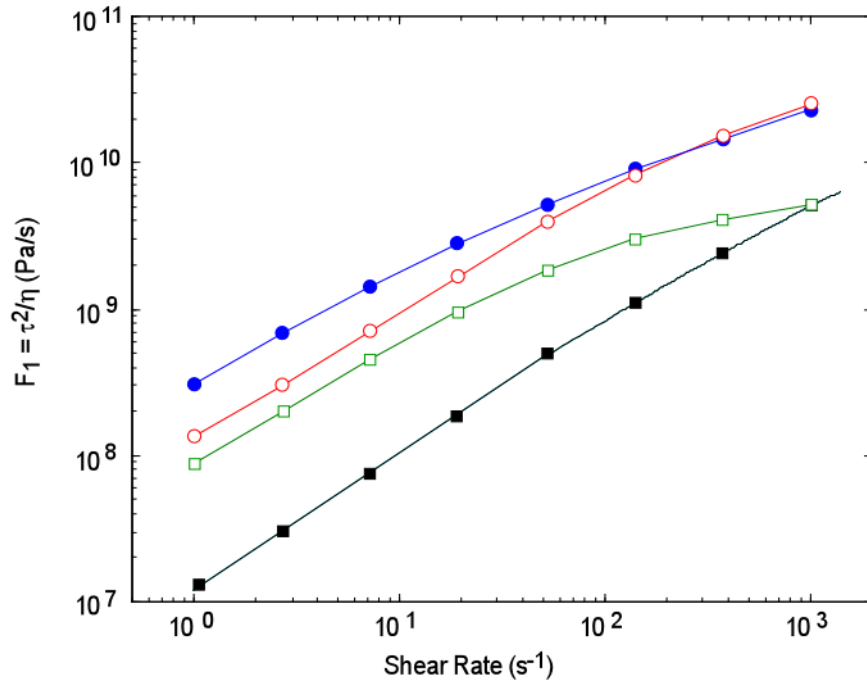


Figure 5. F_1 as a function of shear rate at 25°C and 1.0 Tesla for MRX-126PD (O), MRX-242AS (●), MRX-140ND (□), and MRX-336AG (■).

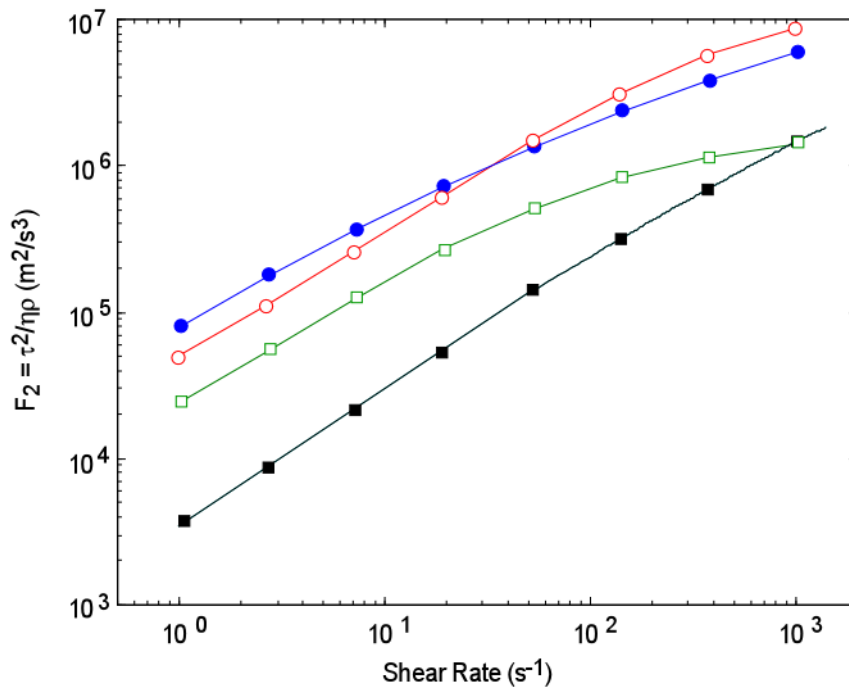


Figure 6. F_2 as a function of shear rate at 25°C and 1.0 Tesla for MRX-126PD (○), MRX-242AS (●), MRX-140ND (□), and MRX-336AG (■).

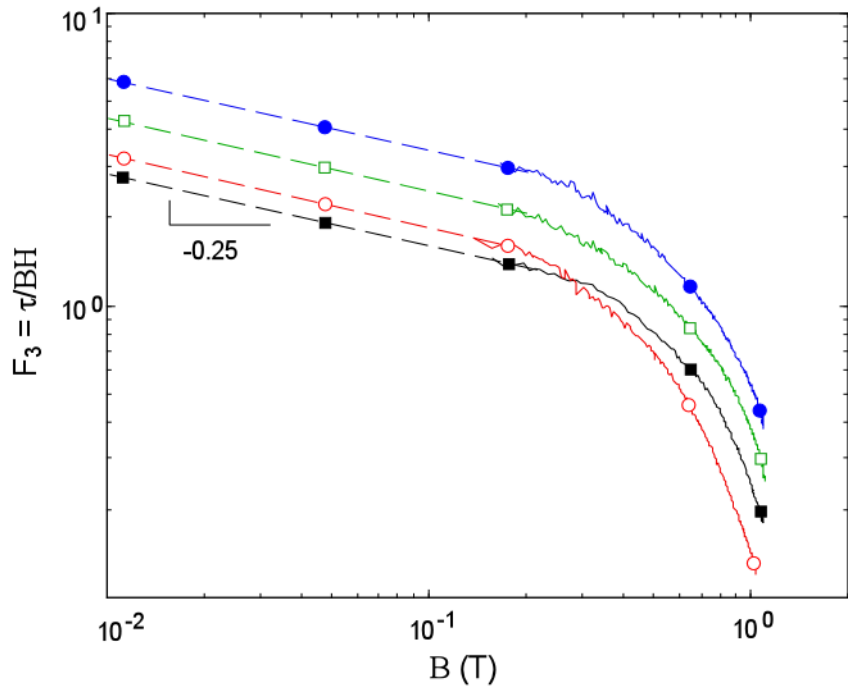


Figure 7. F_3 as a function of flux density at 25°C for MRX-126PD (○), MRX-242AS (●), MRX-140ND (□), and MRX-336AG (■).

4. APPLICATIONS OF COMMERCIAL MR FLUIDS

4.1. Heavy Duty Vehicle Seat Suspensions

Recently a small, monotube MR fluid-based damper (shown in Fig. 8) has been commercialized for use in a semi-active seat suspension system for large on- and off-highway vehicles (Carlson, Catanzarite and St.Clair, 1995; Lord, 1997). In this application the MR damper represents enabling technology for a variety of semi-active control schemes. This damper has also served as a testbed for developing phenomenological device models (Spencer, et al., 1996; Pang et al., 1998).

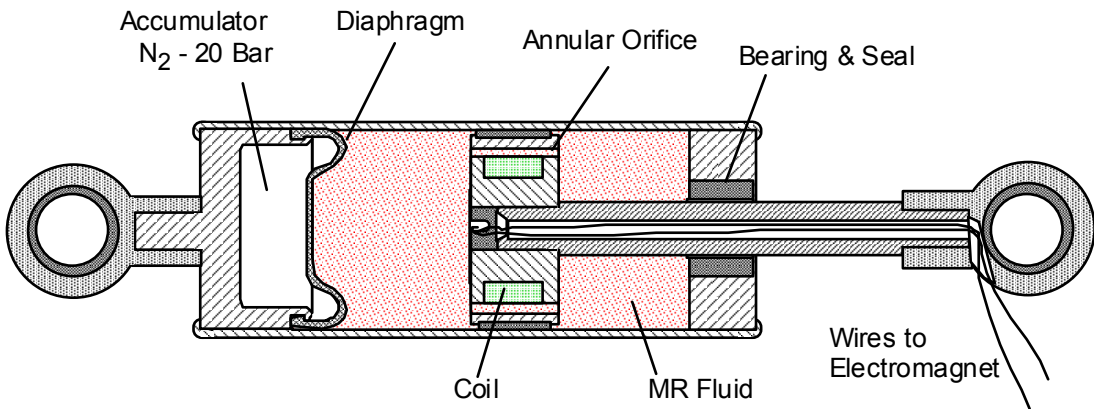


Figure 8. Commercial Linear MR Fluid-based Damper.

The controllable MR damper is capable of providing a wide dynamic range of force control for very modest input power levels as shown in Figure 9. The damper is 4.1 cm in diameter, has a 17.9 cm eye-to-eye length at mid-stroke and has a ± 2.9 cm stroke. The MR fluid valve and associated magnetic circuit is fully contained within the piston. Current is carried to the electromagnetic coil via the leads through the hollow shaft. An input power of 5 watts is required to operate the damper at its nominal design current of 1 amp. Although the damper contains about 70 cm³ of MR fluid, the actual amount of fluid activated in the magnetic valve at any given instant is only about 0.3 cm³.

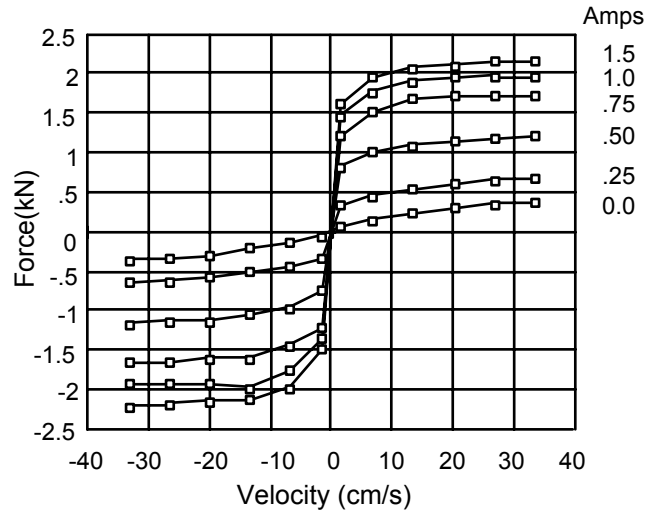


Figure 9. Performance curves for the linear MR damper

This commercial linear MR damper has served as a test bed to demonstrate that MR dampers can have long cycle lives with no significant abrasive wear caused by the MR fluid. As part of the standard product test protocol these dampers are routinely operated through 5-10 million cycles without seal failure. This corresponds to a cumulative linear travel of over 250 km. The key to this long life comes from a combination of dynamic seal design, material selection and MR fluid chemistry. MRX-126PD is typical of the type of fluid used in dampers having a dynamic shaft seal. In addition, this fluid is formulated to have a very low viscosity as a very low off-state is necessary in order to effectively implement semi-active control in this application. The combination of carefully chosen particle morphology and highly effective anti-wear ingredients allow MR fluids to be used reliably in conjunction with dynamic seals. This linear MR damper has also served to demonstrate that the stability of the MR fluid suspension is not an issue for this class of device. Even though the MR fluid used in this damper was formulated to have a very low plastic viscosity, particle separation and settling do not present a problem. The additives in the fluid are very effective at preventing caking or particle sedimentation.

4.2. Control of Seismic Vibrations in Structures

To prove the scalability of MR fluid technology to devices of appropriate size for civil engineering applications, a full-scale, MR fluid damper has been designed and built (Carlson and Spencer, 1996, 1997; Dyke et al., 1996). For the nominal design, a maximum damping force of 200,000 N (20-ton) and a dynamic range of ten were chosen. A schematic of the large-scale MR fluid damper is shown in Fig. 10.

The seismic damper uses a particularly simple geometry in which the outer cylindrical housing is part of the magnetic circuit. The effective fluid orifice is the entire annular space between the piston outside diameter and the inside of the damper cylinder housing. Movement of the piston causes fluid to flow through this entire annular region. The damper is double-ended, i.e. the piston is supported by a shaft on both ends. This arrangement has the advantage that a rod-volume compensator does not need to be incorporated into the damper, although a small pressurized accumulator is provided to accommodate thermal expansion of the fluid. The damper has an inside diameter of 20.3 cm and a stroke of ± 8 cm. The electromagnetic coil is wound in three sections on the piston. This results in four effective valve regions as the fluid flows past the piston. The coils contain a total of about 1.5 km of magnetic wire. The completed damper is approximately 1 m long and with a mass of 250 kg. The damper contains approximately 5 liters of MR fluid. The amount of fluid energized by the magnetic field at any given instant is approximately 90 cm^3 .

Unlike the vehicular seat damper described above which experiences a very lively dynamic environment, the seismic damper is (hopefully) quiescent for most of its life. Such a damper could reasonably be expected to do virtually nothing for many years. However, when a seismic event does occur it must be able to function without hesitation. Such a mode of operation means that one cannot rely on dynamic stroking of the damper to provide any mixing action to maintain a well dispersed fluid. Rather, the fluid must not exhibit significant settling or separation over extended periods of time. MRX-140ND is an MR fluid designed for use in such a seismic damper. Rather than being a totally free flowing liquid, this MR fluid is purposely formulated to have a small but significant yield strength in its off-state. This gives the fluid a custard-like or very soft grease-like consistency which prevents the particles from gravitational settling. As the damper may only experience a few hundred cycles during a seismic event having a duration of one or two minutes, seal life and wear are minor considerations.



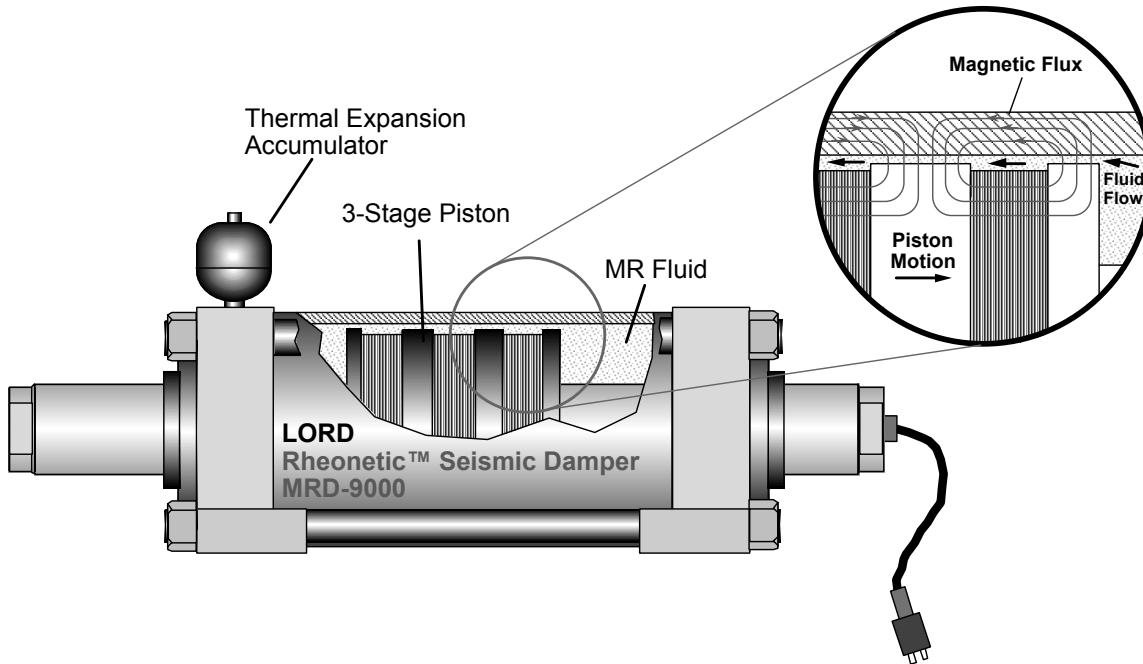


Figure 10. Schematic of MR fluid seismic damper

4.3 “Seal-Less” Vibration Damper

A small, controllable MR fluid vibration damper that is being used for real-time, active-control of damping in industrial applications is shown in Figure 11 (Carlson, Catanzarite and St.Clair, 1995). The damper functions by moving a small steel disk or baffle in a chamber of MR fluid. Primary controlled motion is axial although secondary lateral and flexing motions may also be accommodated. Damping forces of 0 to ± 125 N are produced in the primary direction. This damper may be also be used as a locking device. This damper does not require dynamic, sliding seals. The relatively small amplitudes encountered (± 3 mm) allow the use of elastomeric rubber elements instead. Typically these dampers are used as controllable dashpots in parallel with separate spring elements. Stiffness may also be added to the elastomeric elements so that the damper functions as a controllable mount.

Because this damper is totally sealed, a water-based MR fluid may be used. This is highly desirable as the natural rubber diaphragms are not compatible with the more common hydrocarbon oil based fluids. Water-based fluids can be made exceptionally stable because of the very wide choice of water soluble stabilizers and surfactants that are available. Unfortunately, their use in long-stroke dampers having dynamic seals is precluded however because the microscopic film of water that wets the shaft evaporates slightly on every cycle and eventually leaves the damper dry. Water-based fluids having a consistency of a light thixotropic paste such as MRX-242AS work exceptionally well in small sealed devices of this type.

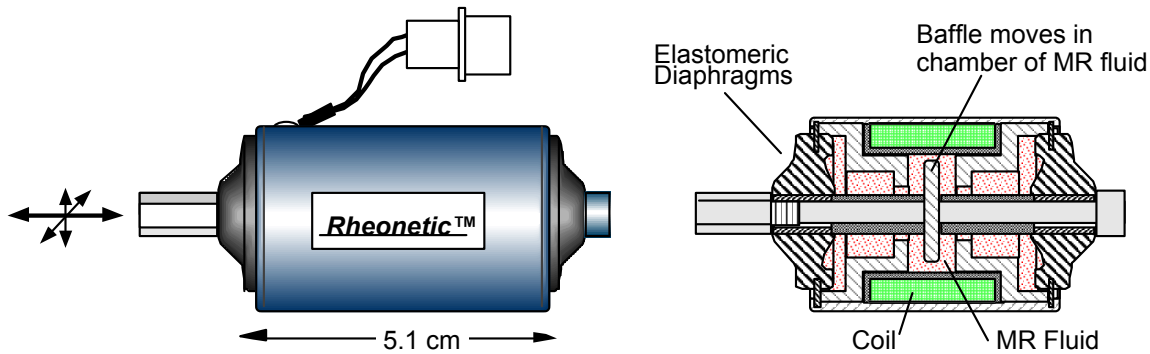


Figure 11. Schematic of small MR fluid vibration damper.

5. CONCLUSIONS

The rheological, magnetic, and material properties of four commercial MR fluids have been presented. Several figures of merit for MR fluids based on these properties were also computed and presented. The examples presented illustrate that the properties and attributes of commercially available MR fluids are wide-ranging. Some of these attributes are summarized in Table 5. It is evident that MR fluids have evolved from laboratory curiosity to true engineering materials that involve engineering trade-offs. The formulation of MR fluids involves the optimal balancing of properties for particular applications or class of applications. Several applications were discussed to illustrate how various material properties may be balanced.

Table 5. Ranking of fluids on the basis of various material properties, with '1' being best or highest and '4' being worst or lowest.

<i>Fluid</i>	τ^2/η	$\tau^2/\eta\rho$	τ/BH	<i>Initial Settling</i>	<i>Friction coefficient</i>	<i>Temper. Range</i>	<i>Compatibility with...</i>	
							<i>Nat. Rubber</i>	<i>Silicone</i>
MRX-126PD	2	2	4	4	1	3	4	3
MRX-140ND	3	3	2	3	2	2	3	2
MRX-242AS	1	1	1	2	3	4	2	1
MRX-336AG	4	4	3	1	4	1	1	4

6. REFERENCES

- Anon., 1995, "Brake cuts exercise-equipment cost," *Design News*, Dec. 4.
- Carlson, J. D. *et al.*, 1994, "Magnetorheological Fluid Dampers", U.S. Patent 5,277,282. (1994) and "Magnetorheological Fluid Devices", U.S. Patent 5,284,330.
- Carlson, J. D., 1994, "The Promise of Controllable Fluids", *Actuator 94, 4th Int. Conf. on New Actuators*, eds. H. Borgmann and K. Lenz, Axon Technologies Consult GmbH, 1994, 266-270.
- Carlson, J. D. and K. D. Weiss, 1994, "A Growing Attraction To Magnetic Fluids", *Machine Design*, Aug. 8 61-66.
- Carlson, J. D., D. M. Catanzarite and K. A. St. Clair, 1995, *5th Int. Conf. on Electrorheological, Magneto-rheological Suspensions and Associated Technology*, Sheffield, July.
- Carlson, J.D. and Spencer Jr., B.F., 1996, "Magneto-Rheological Fluid Dampers for Semi-Active Seismic Control", *Proc. 3rd Int. Conf. on Motion and Vib. Control*, Chiba, JP, Vol. III, pp. 35-40.
- Carlson, J.D. and Spencer Jr., B.F., 1997, "Magnetorheological Fluid Dampers for Seismic Control", *Proc. of DETC'97*, ASME, Sacramento, VIB4124.
- Chase, V.D., 1996, "Cutting Edge," *Appliance Manufacturer*, May, pp. 6.
- Duclos, T.G., 1988, "Design of Devices Using Electrorheological Fluids" *SAE Paper 881134, Future Transp. Techn. Conf. and Exp.*, San Francisco, CA, Aug. 8-11.
- Dyke, S.J., B.F. Spencer, M.K. Sain and J.D. Carlson, 1996, "Seismic Response Reduction Using Magnetorheological Dampers," *Proc. of the IFAC World Congress*, San Francisco, CA.
- Ginder, J.M., L.C. Davis and L.D. Elie, 1995, "Rheology of Magnetorheological Fluids: Models and Measurements," *5th Int. Conf. on ERF, MRS and Their Applications*, July, 1995, Univ. Sheffield, UK.
- Jolly, M. R. and J. D. Carlson, 1996, "Controllable Squeeze Film Damping Using Magnetorheological Fluid" *Actuator 96, 5th Int. Conf. on New Actuators*, eds. H. Borgmann and K. Lenz, Axon Technologies Consult GmbH.
- Jolly, M. R., J. D. Carlson and B. C. Muñoz, 1996, "A Model of the Behaviour of Magnetorheological Materials," *Smart Mater. Struct.* **5**, 607-614.
- Kordonsky, W., 1993, "Magnetorheological Effect As a Base of New Devices and Technologies", *J. Mag. and Mag. Mat.*, **122**, 395-398.
- Kormann, C., M. Laun and G. Klett, 1994, *Actuator 94, 4th Int. Conf. on New Actuators*, eds. H. Borgmann and K. Lenz, Axon Technologies Consult GmbH, 271.
- Lord, 1997, Lord Corporation *Rheonetic Linear Damper - RD-1001/RD-1004 Product Information Sheet*, (Lord Corp. Pub. No. PS RD-1001/4).
- Lord, 1998, www.mrfluid.com
- Nakano, M., H. Yamamoto and M.R. Jolly, 1997, "Dynamic Viscoelasticity of a Magnetorheological Fluid in Oscillatory Slit Flow," *6th Int. Conf. on ERF, MRS and Their Applications*, 22-25 July, 1997, Yonezawa, JP.
- Pang, L., G.M. Kamath and N.M. Wereley, 1998, "Analysis and Testing of a Linear Stroke Magnetorheological Damper," *AIAA/ASME Adaptive Structures Forum*, Paper No. AIAA 98-2040, Long Beach, CA, April, 1997.
- Phillips, R. W., 1969, "Engineering Applications of Fluids with a Variable Yield Stress", Ph.D. Thesis, University of California, Berkeley .
- Rabinow, J., 1948, "The Magnetic Fluid Clutch", *AIEE Trans.*, **67** 1308-1315.
- Rabinow, J., 1948, "Magnetic Fluid Clutch", *National Bureau of Standards Technical News Bulletin*, **32**(4) 54-60.
- Rabinow, J., 1951, "Magnetic Fluid Torque and Force Transmitting Device", U.S. Patent 2,575,360.
- Shtarkman, E.M., 1991, U.S. Patent 4,992,360 (1991) and U.S. Patent 5,167,850 (1992).
- Spencer, B.F., S.J. Dyke, M.K. Sain and J.D. Carlson, 1996, "Nonlinear identification of semi-active

control devices,” *ASCE Eng. Mech. Conf.*, May, 1996.

Weiss K. D. *et al.*, 1993, "High Strength Magneto- and Electro-rheological Fluids", *Society of Automotive Engineers*, SAE Paper # 932451.

Weiss, K.D., J.D. Carlson and D.A. Nixon, 1994. "Viscoelastic Properties of Magneto- and Electro-Rheological Fluids," *J. Intell. Mater. Syst. and Struct.* **5**, 772-775.